Cell Motility and the Cytoskeleton 66: 121–128 (2009)

Guiding Cell Migration in 3D: A Collagen Matrix with Graded Directional Stiffness

Ektoras Hadjipanayi, Vivek Mudera, and Robert A. Brown*

University College London (UCL), Tissue Repair and Engineering Centre, Division of Surgical and Interventional Sciences, Institute of Orthopaedics, Stanmore Campus, London, HA7 4LP, United Kingdom

While matrix stiffness has been implicated in cell adhesion and migration, most studies have focused on the effects of substrate stiffness in 2D. The present work describes a novel continuous stiffness gradient model for studying such processes in 3D. Wedge-shaped collagen scaffolds were compressed to produce sheets of a desired (0.1 mm) uniform thickness, but with increasing collagen density along the length of the sheet. Dynamic mechanical analysis, carried out on 1 mm wide strips obtained from the two ends and the middle of each sheet, showed that the elastic modulus increased from 1057 ± 487 kPa to 2305 ± 693 kPa at the soft and stiff end respectively and was 1835 ± 31 kPa in the middle. In constructs seeded with agarose marker beads prior to compression, mean agarose bead density rose from 10 ± 1 to 71 ± 12 at the soft and stiff end respectively and was 19 ± 5 in the middle, indicating successful engineering of a density gradient corresponding to the measured stiffness gradient. Growth-arrested human dermal fibroblasts, initially seeded evenly within such constructs, accumulated preferentially towards the stiff part of the gradient after 3 and 6 days in culture. Durotactic migration was significant after 6 days. This model provides a new means for studying cellular mechanotaxis and patterning cells which is controllable, biomimetic and in 3D. Cell Motil. Cytoskeleton 66: 121–128, 2009.

Key words: fibroblast; extracellular matrix; stiffness gradient; mechanotaxis

INTRODUCTION

Understanding the mechanisms of cell guidance would provide an invaluable tool for understanding tissue-cell physiology, designing biomimetic structures and engineering tissues. It is already well established that directional movement of cells is an important component of developmental patterning, wound healing and tumor metastasis [Bernstein and Liotta, 1994; Friedl et al., 1998]. While cells migrate in response to cues such as gradients of soluble chemoattractants [Grinnell et al., 2006; Schor et al., 2006], they also appear to receive additional signals from the insoluble ECM. Changes in bound adhesive ligands, topographical features, and stiffness across a substrate are all thought to guide the migration of cells [Brandley and Schnaar, 1989; Huttenlocher et al., 1995; Mandeville et al., 1997; Rajnicek et al., 1997; Lo and Wang, 1999].

The use of patterned adhesivity and topography to organize cells is now a widely used strategy in tissue engineering. When substrates are patterned with ECM coated regions and nonadhesive regions, cells only attach to the ECM-coated regions [Chen et al., 1998], while cells exposed to a gradient of immobilized ECM proteins migrate up the gradient (haptotaxis) [Carter, 1967; Brandley and Schnaar, 1989]. Cells also organize and align in response to topological cues, including surface grooves and ridges (substrate guidance) [Rajnicek et al.,

Contract grant sponsor: BBSRC/ERSPC.

*Correspondence to: Robert A. Brown, UCL-TREC, Institute of Orthopaedics, RNOH, Stanmore Campus, London, HA7 4LP, United Kingdom. E-mail: rehkrab@ucl.ac.uk

Received 13 May 2008; Accepted 21 November 2008

Published online 23 January 2009 in Wiley InterScience (www.interscience.wiley.com).
DOI: 10.1002/cm.20331

1997]. However, in contrast to the maturity of engineering surface adhesivity and topography, methods based on controlled substrate stiffness, and the resulting cellular responses, are only now being developed [Gray et al., 2003; Loftis et al., 2003; Gaudet et al., 2003; Yeung et al., 2005; Ghosh et al., 2007].

A recent study based on an ECM composed of hyaluronan and fibronectin, found that adult human dermal fibroblasts migrate faster on softer substrates and demonstrate more dynamic lamellipodia activity [Ghosh et al., 2007]. Perhaps more significantly, in addition to having an effect on the speed of migration, substrate stiffness has also been implicated in controlling the direction of cell movement. A previous report suggested that cells migrate preferentially towards stiffer surfaces, a phenomenon termed durotaxis [Lo et al., 2000]. In this study, cells were seeded at low density to reduce interfering of cell-cell contacts. Another study of mechanotaxis, using polymeric cell culture surfaces containing micrometer-scale regions of variable stiffness, showed that over several days fibroblasts and endothelial cells accumulated preferentially on stiffer regions of substrates, even in the presence of cell-cell contacts [Gray et al., 2003]. A distinct feature of these studies is the use of polyacrylamide/PDMS surfaces of varying stiffness [Pelham and Wang, 1998; Gray et al., 2003; Saez et al., 2007] which introduces two major limitations in terms of experimental design. Primarily, cells are seeded on a surface and not within a physiological three dimensional environment. Any observations of cellular response thus have to be critically examined in the scope of engineering three dimensional structures. In addition, most of these patterned surfaces present the cells with sharp boundaries between soft and stiff regions (step gradient) instead of a smooth gradient as is the case with chemotactic signaling.

This work describes a novel model of a 3D continuous stiffness gradient engineered within collagen scaffolds and tests the hypothesis that cell migration will be guided by such a gradient. Characterization of this 3D durotactic gradient in a collagen matrix may clarify our understanding of physiological cell movement, for example in tissue repair, and inform the design of new engineered tissue models.

MATERIALS AND METHODS

Fabrication of Collagen Constructs with Graded Stiffness

Collagen gels were prepared as previously described. Briefly, a collagen gel mixture composed of 5.6 ml acid soluble collagen type I (2.20 mg/ml; First Link, UK) and 1.4 ml 10× Dulbecco's modified Eagle's medium (DMEM) (Gibco Life Technologies, UK) was neutralized by 235.5 μl of 5 M NaOH. Collagen constructs with a gradient of biomaterial matrix stiffness were prepared by casting 7 ml of collagen solution in moulds (4 × 2.5 × 1.1 cm), made from Derlin blocks (Intertech, UK), which were cast at an incline of 15° (Fig. 1a). Collagen gels were incubated at 37°C in a 5% CO_2 humidified incubator for 20 min. After setting, the resulting wedge-shaped collagen constructs were compressed vertically by a horizontal plate, moved by a computer controlled motor (Dartec, UK) to produce sheets of (0.1 mm) uniform thickness (Fig. 1b). This compressing stage used the same method as described for plastic compression fabrication of collagen-cell constructs [Brown et al., 2005]. It is important to note that values of final collagen density were calculated based on the final construct thickness, in this case 100 μm, as shown in Fig. 2.

Measurement of Collagen Matrix Young's Modulus

Compressed collagen constructs with a gradient of collagen density were divided equally into three regions, from less to more dense zones. Dynamic mechanical analysis (Perkin Elmer, UK) was carried out on 1 mm wide strips obtained from each region to measure the elastic modulus and thus the rigidity gradient that formed from the compliant to the stiff end of the construct [Brown et al., 2005]. Strips were uniaxially deformed along their longest axis with the amount of tension required to produce a 5–30% strain. Samples were perfused with phosphate-buffered saline (PBS) between measurements. The stress-strain relationships were linear for the tested samples. Young's modulus was calculated using the formula: $E = (F/A)(L/\Delta L)$, where A = unstressed cross sectional area, F = force, L = unstressed length, and ΔL = change in length. The values reported are the averages of at least three samples from each region.

Quantification of Density Gradient

As a measure of the density gradient resulting after compression, collagen gels were seeded with agarose marker beads (Sigma, UK) (0.15 ml of 0.2 g/ml stock solution) before setting. After compression, each construct was divided in 3 equal areas, corresponding to the soft, middle and stiff parts of the gradient. The number of beads per 10× photographic field was manually counted in each of the three areas, using a phase contrast microscope. Averages based on five fields per area, per construct; 3 constructs were analyzed.

Cell-Seeded Constructs to Test Migration

Adult human dermal fibroblasts (<10 passages) were cultivated in complete culture media composed of DMEM supplemented with 10% (v/v) fetal calf serum

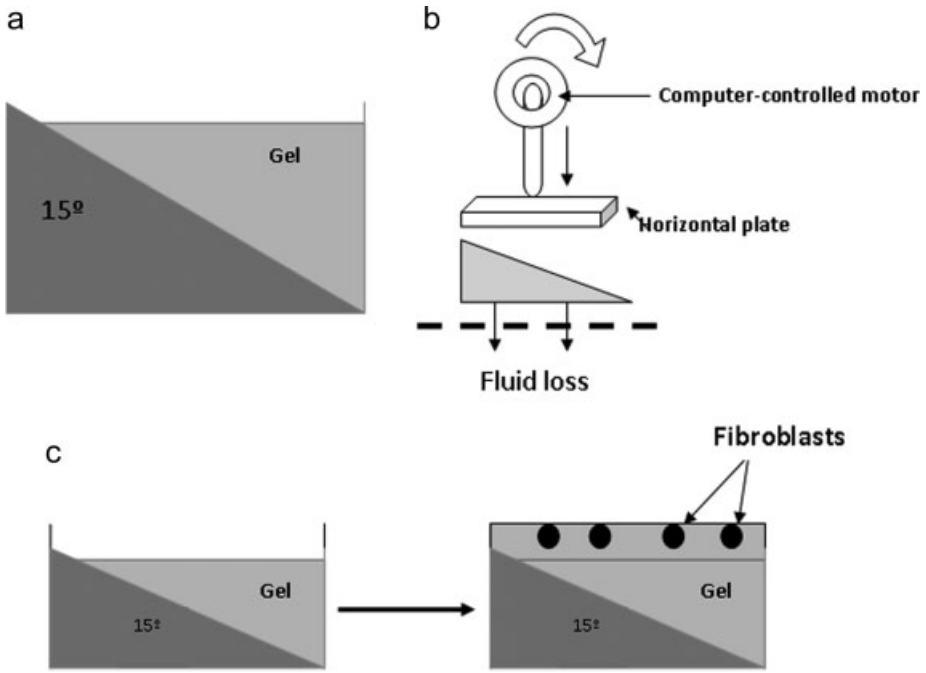

Fig. 1. (**a**) Fabrication of collagen constructs with a gradient of biomaterial matrix stiffness. Collagen solution (light grey area) was casted in moulds (dark grey area) set at an incline of 15°, resulting in formation of wedge-shaped collagen constructs. (**b**) After setting, the wedge-shaped collagen constructs were compressed vertically by a horizontal plate, moved by a computer-controlled motor, to produce sheets of (0.1 mm) uniform thickness. (**c**) Cell-seeded constructs were fabricated by first pouring 5 ml of acellular collagen solution and after 1 min pouring a second layer of cell-containing collagen solution (2 ml). This ensured even distribution of cells, resulting in a uniform cell density along the construct after compression.

(FCS, First Link, UK), 2 mmol/l glutamine (Gibco Life Technologies, UK), 1,000 U/ml penicillin and 100 mg/ml streptomycin (both from Gibco Life Technologies, UK). Cell-seeded collagen constructs were prepared by first casting 5 ml of acellular collagen solution and after 1 min, before the collagen had set, casting a second layer of collagen solution (2 ml) containing a total of 20,000 fibroblasts (Fig. 1c). The short duration between casting the first 5 ml and final cell-seeded 2 ml of collagen solution ensured adequate integration across the interface of the two layers [Hadjipanayi et al., 2008] so that after setting, a single collagen construct was obtained with no obvious line of separation. This method resulted in collagen constructs having a uniform fibroblast density (2000 cells/cm^2) after compression. Seeding the whole collagen construct with cells was avoided, since this also generated a cell density gradient, due to accumulation of cells towards the thick end of the wedge. After casting, wedge-shaped cell-seeded constructs were compressed to produce sheets of (0.1 mm) uniform thickness, as described above. Cells were growth arrested by 10 μg/ml of mitomycin C (Sigma, UK), which was left in the culture media for 2 h after cell seeding and removed by three washes of PBS. Collagen constructs were cultured at 37°C for up to 6 days, with replacement of culture media (5 ml) every second day.

Quantification of Cell Accumulation

Collagen constructs were taken out of culture after 0, 3 and 6 days of culture and incubated for 1 h in PBS plus 5 μM calcein AM (Molecular Probes, Invitrogen) at 37°C. Samples were subsequently washed in PBS and viewed with a fluorescence microscope. Cells were counted manually. Each construct was divided into three equal regions (stiff, middle, soft) and cell density within each region was calculated as the average number of cells per 10× photographic field. Since cells had moved across a 3D space within the construct, the plane of focus was manually set and kept constant during counting. Reported values are averages of five fields per region per construct with three constructs per time point.

Statistical Analysis

For each experimental condition a sample size of three or more was used. Data is expressed as mean± standard deviation. Statistical analysis was carried out using one-way ANOVA (or Kruskal-Wallis test for nonparametric distribution) accompanied with multiple

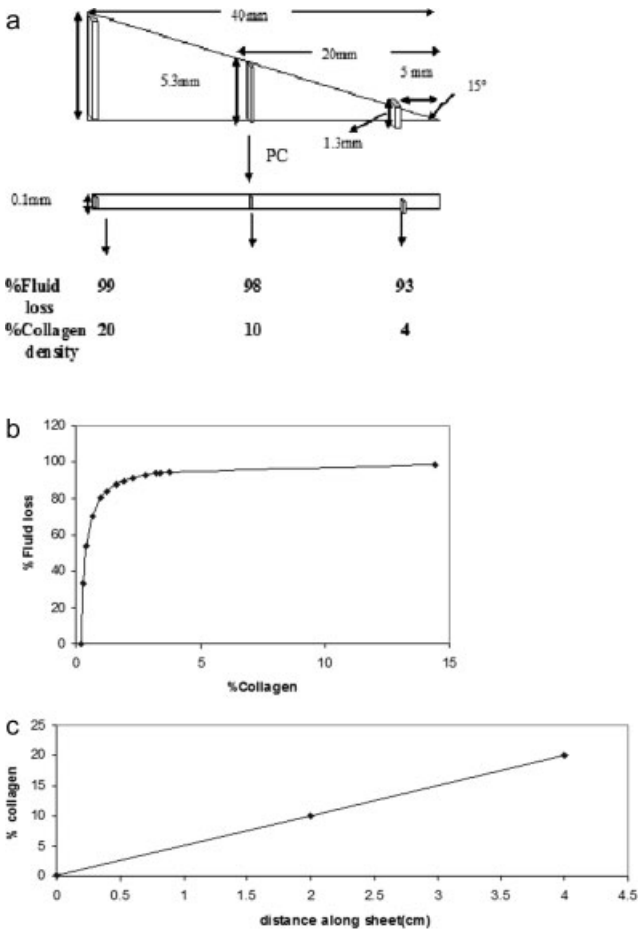

Fig. 2. (**a**) Schematic showing how the % fluid loss and % collagen density at the two ends and middle region of a construct can be calculated. Angle of inclination of the mould used to set the collagen gel was 15°. Compression was to a controlled final thickness of 0.1 mm. (**b**) Plot of % fluid loss against % collagen density during compression of a collagen gel with initial collagen density of 2 mg/ml (0.2%). (**c**) Plot showing how % collagen density varies with distance along a collagen sheet compressed to 0.1 mm.

comparison tests, using SPSS 14 software. Differences were considered significant when $P < 0.05$.

RESULTS

We hypothesized that vertical compression of collagen gels with a wedge-shaped cross section, by a horizontal plate, must leave more collagen material at one end (thick end of the wedge) than the other and so produce an increasing density along the length of the construct. Production of a flat wedge surface will produce a linear gradient (rate of change proportional to the angle of that surface). However, nonlinear (e.g. exponential) density gradients could be formed by casting the gel surface in a curved profile.

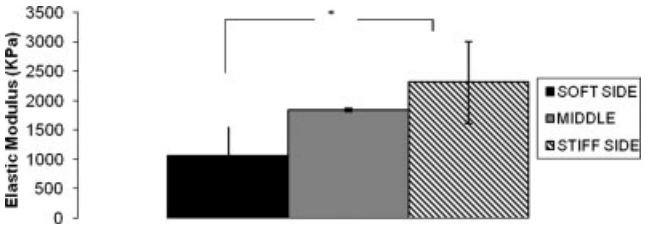

Fig. 3. Young's moduli for the compliant (soft), middle and stiff regions of the construct, as measured by dynamic mechanical analysis. The >2-fold increase between the compliant and stiff ends was significant (*$P < 0.05$).

In order to quantify this stiffness gradient we measured the elastic modulus at the two extreme ends and in the middle of the compressed sheet. This was measured by loading 1 mm wide strips of these three construct regions, perpendicular to the axis of the density gradient, using the DMA. The Young's modulus increased from 1057 ± 487 kPa at the soft end to 2305 ± 693 kPa at the stiff end ($P < 0.05$) and was 1835 ± 31 kPa in the middle. This represented a near linear increase in modulus along the construct (Fig. 3).

Uncompressed constructs were seeded with agarose marker beads in order to quantify the density gradient which generated this stiffness gradient. Seeding the constructs with marker beads also aimed to mimic the cellular density gradient that would form if the constructs were cell-seeded. The use of agarose beads, instead of cells, eliminated any complications due to changes in cell morphology, cell movement during processing or cell-mediated collagen contraction. Mean agarose bead density along this gradient rose from 10 ± 1 to 71 ± 12 from the soft to stiff ends respectively and was 19 ± 5 in the middle (Fig. 4a, and 4b). This indicated successful engineering of a density gradient and partly corresponding to the stiffness gradient measured. The nonlinear rise in bead density (contrast with linear increase in modulus) is likely to be a result of beads tending to settle under gravity and accumulate towards the thick lower end of the wedge during the short gelation period. A comparable nonlinear shift would be expected for cell seeded gels, though its magnitude would probably be less and dependent on cell type and gelling conditions.

To test the hypothesis that such 3D gradients could direct cell migration, cells were seeded in constructs with a rigidity gradient of 1057 ± 487 kPa to 2305 ± 693 kPa, from the soft to the stiff end respectively (over 40 mm length), and cultured over 3 and 6 days. Human dermal fibroblasts, treated with mitomycin C to block proliferation [Daniels et al., 1999; Nieto et al., 2007], were seeded at low density (2,000 cells/cm^2) in wedge-

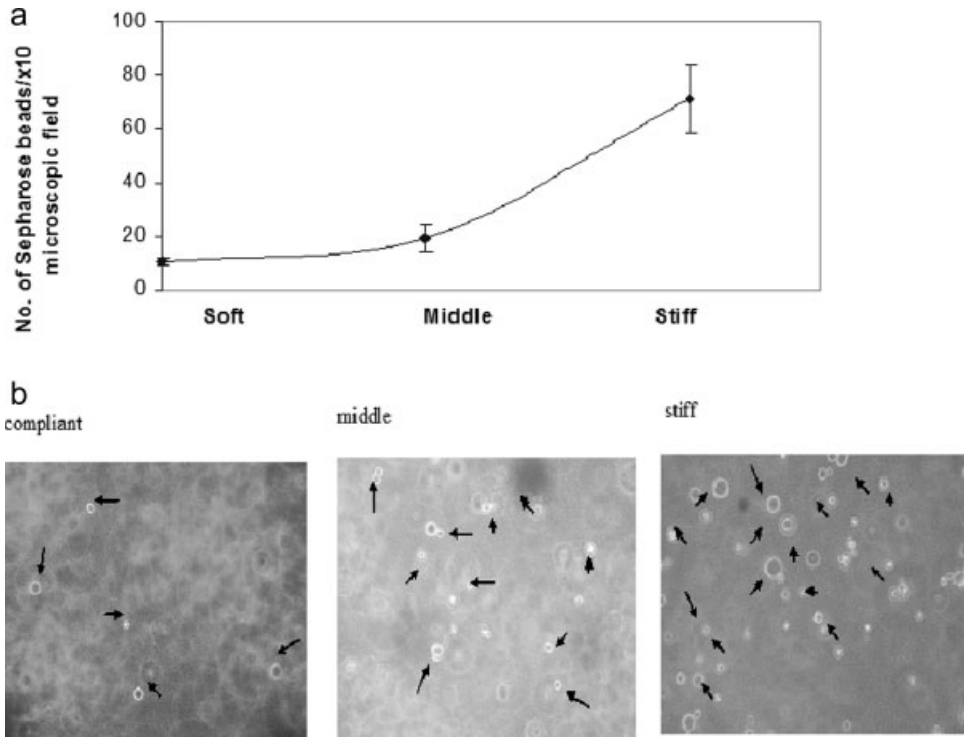

Fig. 4. (**a**) Agarose marker beads in the soft, middle and stiff areas of the construct, as a measure of the density gradient. Readings are average number of beads per ×10 photographic field, 5 fields per area per construct, 3 constructs tested. (**b**) Phase contrast images (×10) of the soft, middle and stiff areas of the construct. Arrows show agarose beads.

shaped collagen constructs, using a 2 stage casting process (Fig. 1c), so that cell density was uniform along the gradient at $t = 0$. Importantly, at this low seeding density, cell-cell contact was seen to be minimal. Average cell density was measured in the compliant, middle and stiff regions of the construct at 3 and 6 days of culture. Although there was a trend for preferential accumulation of cells towards the stiff region of the gradient at 3 days of culture, this only reached statistical significance after 6 days ($P < 0.05$) (Fig. 5). This system produced a final difference in cell density across the gradient of threefold. This relatively slow rate of cell re-positioning is likely to be due to the high substrate density at the extreme which would retard cell locomotion. It is important to note that the increase in the average cell density in the stiff region was accompanied by a decrease in the compliant region, implying that cells migrated out of the soft and into the stiffer regions. Since the cells were growth-arrested, migration and not proliferation was responsible for this directional accumulation. Indeed, the average cell density within each construct did not significantly differ between day 0, 3, and 6 days of culture ($P > 0.05$), establishing that the fall in cell density in the soft region was not a result of cell death.

DISCUSSION

We have successfully engineered a model of a three dimensional continuous stiffness gradient based on collagen. Previous studies of mechanotaxis have focused on culturing cells on two dimensional patterned substrates [Lo et al., 2000; Gray et al., 2003; Ghosh et al., 2007]. In addition to their limitations as biomimetic models of cell function in 3D, the use of polyacrylamide as the scaffold is also poorly biomimetic. In this study the choice of collagen, the most abundant protein component of the ECM, enabled the development of a biomimetic environment which is truly 3D.

In our model, casting preparation of the collagen gel scaffold is an one-step process, in contrast to that for synthetic polymer surfaces [Gray et al., 2003], with rapid fabrication of a density gradient. The density gradient nature of this model also has the advantage of exposing cells to a continuous stiffness gradient in contrast to sharp boundaries of changing material stiffness in previous studies [Gray et al., 2003].

It was possible to quantify this stiffness gradient by measuring the stiffness modulus in the compliant, middle and stiff regions of the construct. This gave a >2 fold

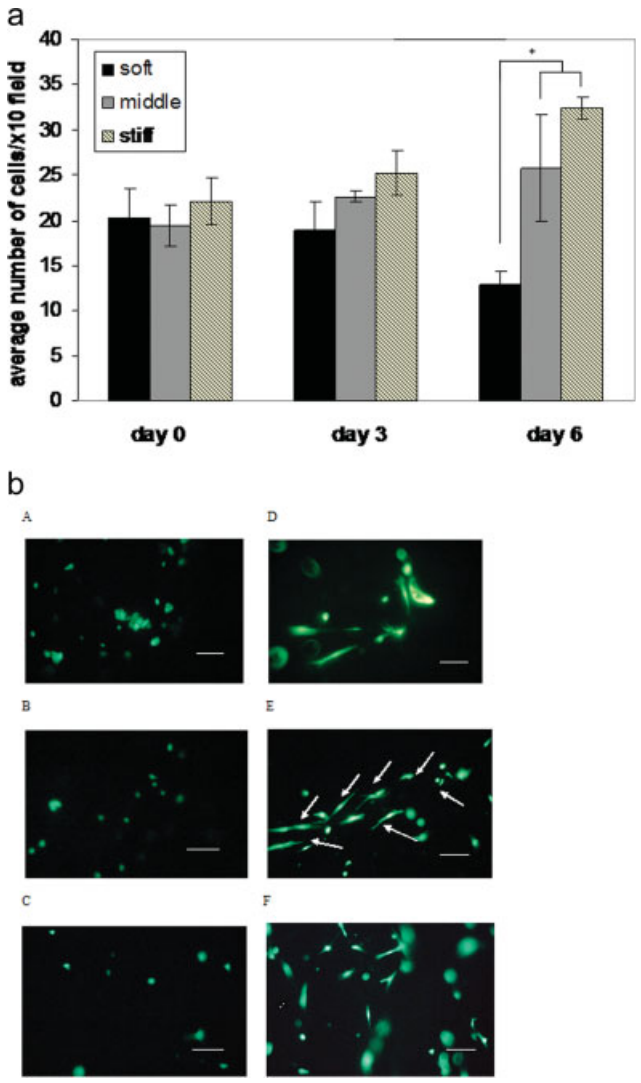

Fig. 5. (**a**) Measurements of the number of cells in the soft, middle and stiff regions of the construct at 0, 3, and 6 days of culture. Contructs were stained with calcein to visualize live cells. Readings are averages of five fields per region per construct with three constructs per time point ($*P < 0.05$). The average cell density within each construct did not significantly differ between day 0 and 3 or 6 days of culture ($P > 0.05$). (**b**) Fluorescence microscopy images ($\times 10$) at day 0 (A–C) and day 6 (D–F) of culture, from the soft (A, D), middle (B, E) and stiff regions of the construct (C, F). Arrows in image E show bipolar, elongate fibroblasts migrating parallel to gradient axis, Bars = 10 μm.

increase in modulus for a fivefold increase in collagen density. The range of matrix stiffness (1 to 2 MPa) tested here was in the native tissue range (e.g. skin, tendon). Varying the final construct thickness by adjusting the degree of compression can predictably change the magnitude of the collagen density gradient and thus the stiffness gradient. For example, matrix stiffness in the range of 20 to 50 kPa could be used to model granulation to scar tissue formation during wound healing [Hinz, 2007]. In addition, the angle of inclination of the casting well will determine the rate of change of stiffness in the gradient corresponding with the collagen density. Indeed, the linearity or nonlinearity of the gradient will be determined by the slope of the inclined surface of the gel (flat or curved). It is important to note that the high end of the stiffness range tested here is only the same as that previously reported [Brown et al., 2005], with no significant cell damage. Therefore, there is presently no reason to expect that cells in different parts of this gradient have been significantly affected (differentially) by the initial compression. In addition, previous studies have found similar cell viability and cellular responses even after double compression, which raises the matrix stiffness dramatically [Bitar et al., 2007].

We also demonstrated the preferential accumulation of cells towards the stiffer regions of the gradient. During cell seeding we employed a two step casting process, in order to produce a uniform cell density along the length of the construct (Fig. 1c). This allowed relative changes in cell density to be quantified. Had we seeded the whole wedge-shape construct with cells, a cell density gradient would have been formed from the start, as shown by the agarose bead experiment. The ability to observe mechanotaxis on a large population over a long period enables a statistical approach to studying the phenomenon in three dimensions and complements the cell by-cell, time-lapse observations that first reported durotaxis [Lo et al., 2000]. Early studies of durotaxis found that isolated cells were able to migrate only from compliant to stiff regions, but that cells with neighbors were able to migrate from stiff to compliant regions as well [Lo et al., 2000]. This is not surprising as the measured migration is likely to be an average of movement events in all directions. The short time scale of these studies and the lack of population data did not enable the clarification of what the net effect would be on the whole population. Our findings are in agreement with that of a previous study that investigated the durotactic migration of larger cell populations in two dimensions [Gray et al., 2003] and show that over a sufficiently long time span and averaged over many cells, a net migration into stiff regions occurs.

In this model the stiffness gradient corresponded to a collagen density gradient, from the compliant to the stiff end of the scaffold. This suggests that an integrin-binding ligand density gradient accompanied the formation of the rigidity gradient, leading to a concurrent gradient adhesiveness, which can also lead to a directed cell motility response (i.e., haptotaxis) [Carter, 1967; Brandley and Schnaar, 1989]. This would imply that preferential accumulation of cells towards the stiff regions of the construct was not entirely caused by durotaxis. However, it has recently been suggested that, physiologically, matrix compliance and ligand density are not mutually exclusive, but

highly coupled (orthogonal) variables that determine mean cell responses ranging from cell spreading to cell shape and molecular organization [Cukierman et al., 2001; Geiger, 2001]. Sensing the stiffness of the substrate is associated with the binding of integrin receptors with ECM proteins that provide anchors to the cytoskeletal network via cytoplasmic scaffolding proteins [Chen et al., 2004]. Using the integrin-mediated mechanosensor, cells can probe the stiffness of the substrate to simply move or pull on their microenvironment. Indeed, it has been shown that smooth muscle cell spreading is driven by intracellular processes such as actin filament growth but modulated by external cues that include substrate stiffness as well as ligand density [Engler et al., 2004].

It has been shown that substrate stiffness can have profound effects on cell proliferation [Wang et al., 2000; Yeung et al., 2005; Ghosh et al., 2007]. In our group we have found that fibroblasts proliferated faster when seeded within stiffer 3D collagen gels [Hadjipanayi et al., 2007]. In order to isolate the migratory response of cells, it was important to exclude these proliferative effects and this was done by treating cells with mitomycin C. Although trends were apparent at 3 days, accumulation of cells in stiff regions only became significant after 6 days of culture. This rate of migration seems to be comparable to the findings of a previous study where significant accumulation was observed after 5 days [Gray et al., 2003]. It is important, however, to note that in our model cells were seeded within a 3D matrix whereas in the previous study they were cultured on a 2D surface and that matrix remodeling during cell locomotion in three dimensions has been shown to have a significant effect on the rate of migration [Ghosh et al., 2007]. In addition to matrix molecular composition and rigidity, the topography (three-dimensionality) of a matrix affects the formation of cellular adhesions [Cukierman et al., 2001]. This is a key point, as physiologically stromal cells must also migrate through the 3D ECM. Furthermore, the 3D matrix stiffness in this model was in the range of 1–2 MPa, compared to previously described 2D substrates, typically in the range of 1–40 kPa [Gray et al., 2003; Ghosh et al., 2007]. Increasing density/stiffness of ECM (and durotactic migration) is accompanied, however, by greater 'matrix drag', as cells must penetrate more dense fibril networks with increasing overall cell adhesiveness and decreasing progression between fibrils. This dimension is key to physiological stromal cell migration as net progression is a balance of these two opposing factors, modified by the ability of the cell type in question to secrete matrix proteases, such as MMPs, and so degrade a pathway or modify a section of ECM. This is supported by the finding that a biphasic dependence of migration speed on ECM stiffness exists, with an optimal substrate stiffness capable of supporting maximal migration [Peyton and Putnam, 2005]. As a result, the ability of cells to optimize migration rate, towards the ideal (durotaxis only) rate will depend on their ability to generate controlled, local proteolytic activity capable of reducing 'matrix drag'. Indeed, we have previously showed that collagen matrix stiffness regulates MMP production by fibroblasts cultured within collagen constructs i.e., MMP secretion is mechanosensitive [Karamichos et al., 2007].

The current model is based on progression through largely homogeneous random (isotropic) collagen fibril meshes, as plastic compression of collagen hydrogels does not result in any significant fibril alignment [Cheema et al., 2007]. However, these are almost never found in native ECM, rather local or long-range fiber alignments produce matrix anisotropies. The presence of fibril alignment on a directional stiffness/density gradient would be expected to generate the highest cell speeds (and so net migration velocities) parallel to fibril alignment or between fibril bundles where 'matrix drag' will be minimal and durotactic advantage maximal. Interestingly, this is consistent with common fibroblast behavior to migrate between existing tissue planes. In this model it is possible that, after extended culture periods, such cell-mediated differential collagen matrix organization [Brown et al., 2005] could have a significant effect on the rate and direction of cell migration. Any such effect would be expected to gradually enhance the initial matrix gradient/anisotropy over extended periods.

Using this model, it will be possible to better understand factors governing the rate and direction of cell migration in tissues where spatiotemporal changes in ECM stiffness occur e.g. during embryonic development or wound healing and tissue repair [Hinz, 2007]. The ability to guide cells in 3D using matrix stiffness gradients could also have important implications for engineering tissue constructs. Matrix stiffness is increasingly recognized as an important regulator of cell proliferation, adhesion and collagen deposition [Ghosh et al., 2007; Hadjipanayi et al., 2007; Karamichos et al., 2007], cellular functions that are critical for biomimetic and functional tissue growth. As discussed above, the current method allows stiffness gradients of variable magnitude to be produced, matching the stiffness of the target tissue e.g. stiffer in bone tissue, elastic in cardiovascular or muscle tissue, and relatively softer in brain or skin tissue. This model could thus be an important tool for designing and engineering tissue implants with a built-in ability to direct cell in growth, accumulation and transit.

CONCLUSION

We have developed a model of a 3D stiffness gradient within a collagen scaffold that will be valuable

for investigation of cellular movement in 3D tissues where ECM stiffness is an important factor, such as embryo development, wound healing and tissue growth, remodeling or aging. Durotactic control of cell migration rate and direction may also be an important tool for engineering biomimetic structure and function into tissue implants or models for screening and research.

REFERENCES

Bernstein LR, Liotta LA. 1994. Molecular mediators of interactions with extracellular matrix components in metastasis and angiogenesis. Curr Opin Oncol 6:106–113.

Bitar M, Salih V, Brown RA, Nazhat SN. 2007. Effect of multiple unconfined compression on cellular dense collagen scaffolds for bone tissue engineering. J Mater Sci: Mater Med 18:237–244.

Brandley BK, Schnaar RL. 1989. Tumor-cell haptotaxis on covalently immobilized linear and exponential gradients of a cell-adhesion peptide. Dev Biol 135:74–86.

Brown RA, Wiseman M, Chuo CB, Cheema U, Nazhat SN. 2005. Ultrarapid engineering of biomimetic materials and tissues: Fabrication of nano- and microstructures by plastic compression. Adv Funct Mater 15:1762–1770.

Carter SB. 1967. Haptotaxis and mechanism of cell motility. Nature 213:256–260.

Cheema U, Chuo CB, Sarathchandra P, Nazhat SN, Brown RA. 2007. Engineering functional collagen scaffolds: Cyclical loading increases material strength and fibril aggregation. Adv Funct Mater 17:2426–2431.

Chen CS, Mrksich M, Huang S, Whitesides GM, Ingber DE. 1998. Micropatterned surfaces for control of cell shape, position, and function. Biotechnol Prog 14:356–363.

Chen CS, Tan J, Tien J. 2004. Mechanotransduction at cell-matrix and cell-cell contacts. Annu Rev Biomed Eng 6:275–302.

Cukierman E, Pankov R, Stevens DR, Yamada KM. 2001. Taking cell-matrix adhesions to the third dimension. Science 294:1708–1712.

Daniels JT, Occleston NL, Crowston JG, Khaw PT. 1999. Effects of antimetabolite induced cellular growth arrest on fibroblast-fibroblast interactions. Exp Eye Res 69:117–127.

Engler A, Bacakova L, Newman C, Hategan A, Griffin M, Discher D. 2004. Substrate compliance versus ligand density in cell on gel responses. Biophys J 86(1 Part 1):617–628

Friedl P, Zanker KS, Brocker EB. 1998. Cell migration strategies in 3-D extracellular matrix: Differences in morphology, cell matrix interactions, and integrin function. Microsc Res Tech 43:369–378.

Gaudet C, Marganski WA, Kim S, Brown CT, Gunderia V, Dembo M, Wong JY. 2003. Influence of type I collagen surface density on fibroblast spreading, motility, and contractility. Biophys J 85:3329–3335.

Geiger B. 2001. Encounters in space. Science 294:1661–1663.

Ghosh K, Pan Z, Guan E, Ge SR, Liu YJ, Nakamura T, Ren XD, Rafailovich M, Clark RAF. 2007. Cell adaptation to a physiologically relevant ECM mimic with different viscoelastic properties. Biomaterials 28:671–679.

Gray DS, Tien J, Chen CS. 2003. Repositioning of cells by mechanotaxis on surfaces with micropatterned Young's modulus. J Biomed Mater Res A 66:605–614.

Grinnell F, Rocha LB, Iucu C, Rhee S, Jiang HM. 2006. Nested collagen matrices: A new model to study migration of human fibroblast populations in three dimensions. Exp Cell Res 312:86–94.

Hadjipanayi E, Mudera V, Brown RA. 2008. Interface integration of rapidly engineered multi-layer collagen scaffolds. Tissue Eng 14:748.

Hadjipanayi E, Mudera V, Brown RA. 2007. Close dependence of fibroblast growth on collagen scaffold matrix stiffness. Tissue Eng 13:1657.

Hinz B. 2007. Formation and function of the myofibroblast during tissue repair. J Invest Dermatol 127:526–537.

Huttenlocher A, Sandborg RR, Horwitz AF. 1995. Adhesion in cell-migration. Curr Opin Cell Biol 7:697–706.

Karamichos D, Brown RA, Mudera V. 2007. Collagen stiffness regulates cellular contraction and matrix remodelling gene expression. J Biomed Mater Res A 83:887–894.

Lo CM, Wang YL. 1999. Guidance of cell movement by substrate rigidity. Mol Biol Cell 10:259A.

Lo CM, Wang HB, Dembo M, Wang YL. 2000. Cell movement is guided by the rigidity of the substrate. Biophys J 79:144–152.

Loftis MJ, Sexton D, Carver W. 2003. Effects of collagen density on cardiac fibroblast behavior and gene expression. J Cell Physiol 196:504–511.

Mandeville JTH, Lawson MA, Maxfield FR. 1997. Dynamic imaging of neutrophil migration in three dimensions: Mechanical interactions between cells and matrix. J Leukoc Biol 61:188–200.

Nieto A, Cabrera CM, Catalina P, Cobo F, Barnie A, Cortes JL, del Jesus AB, Montes R, Concha A. 2007. Effect of mitomycin-C on human foreskin fibroblasts used as feeders in human embryonic stem cells: Immunocytochemistry MIB1 score and DNA ploidy and apoptosis evaluated by flow cytometry. Cell Biol Int 31:269–278.

Pelham RJ, Wang YL. 1998. Cell locomotion and focal adhesions are regulated by the mechanical properties of the substrate. Biol Bull 194:348–349.

Peyton SR, Putnam AJ. 2005. Extracellular matrix rigidity governs smooth muscle cell motility in a biphasic fashion. J Cell Physiol 204:198–209.

Rajnicek AM, Britland S, Mccaig CD. 1997. Contact guidance of CNS neurites on grooved quartz: Influence of groove dimensions, neuronal age and cell type. J Cell Sci 110:2905–2913.

Saez A, Ghibaudo M, Buguin A, Silberzan P, Ladoux B. 2007. Rigidity-driven growth and migration of epithelial cells on microstructured anisotropic substrates. Proc Natl Acad Sci USA 104:8281–8286.

Schor SL, Ellis IR, Harada K, Motegi K, Anderson ARA, Chaplain MAJ, Keatch RP, Schor AM. 2006. A novel 'sandwich' assay for quantifying chemo-regulated cell migration within 3-dimensional matrices: Wound healing cytokines exhibit distinct motogenic activities compared to the transmembrane assay. Cell Motil Cytoskeleton 63:287–300.

Wang HB, Dembo M, Wang YL. 2000. Substrate flexibility regulates growth and apoptosis of normal but not transformed cells. Am J Physiol Cell Physiol 279:C1345–C1350.

Yeung T, Georges PC, Flanagan LA, Marg B, Ortiz M, Funaki M, Zahir N, Ming WY, Weaver V, Janmey PA. 2005. Effects of substrate stiffness on cell morphology, cytoskeletal structure, and adhesion. Cell Motil Cytoskeleton 60:24–34.